

24th COBEM - 2017



24th ABCM International Congress of Mechanical Engineering
December 3-8, 2017, Curitiba, PR, Brazil

COBEM-2017-0606

ENERGY BALANCE APPROACH TO ANALYZE CRANKSHAFT DEEP ROLLING SIMULATION RESULTS

Luiz Guilherme Aun Fonseca

Alfredo Rocha de Faria

Instituto Tecnológico de Aeronáutica, Mechanical Engineering Division, São José dos Campos, SP, Brazil

luizaun@ita.br

arfaria@ita.br

Abstract. *The results of deep rolling process made on crankshafts are still not fully understood to this day. Understanding and correctly simulating the process dynamics is key to investigate process influence on material microstructure. A numerical model using an explicit formulation was developed in order to accurately simulate deep rolling dynamics. Real boundary conditions, contact and converged mesh were set. The results were evaluated in terms of energy balance output. Conclusions can be drawn on the accuracy of the model representation of the real process based on this analysis.*

Keywords: *crankshaft, deep rolling, energy balance, explicit formulation*

1. INTRODUCTION

Deep rolling is performed on crankshafts since the 1960's and has approximately 75% of the market share for passenger car engine crankshafts according to information brought by (C. Cevik 2011). Yet there is still a knowledge gap concerning what is happening to the target surface microstructure. Deep rolling, as a forming process, introduces residual stresses to the fillet radii of main bearings and crankpins to increase fatigue material strength in these particular areas. There is no consolidated numerical method for prediction of the outcomes from this manufacturing process. This research investigates the energy output from a proposed simulation of deep rolling in order to set the foundations of a method to be applied in general cases.

Research on the process numerical modeling and simulation are still at an early stage. A two-dimensional model was developed by (Choi and Pan 2005) and used by (Chien et al. 2005) and (Choi and Pan 2009) to investigate deep rolling parameters and its influence on compressive stress state after process. The two-dimensional model, however, does not take the process kinematics in consideration, but only applies the rolling force to the crankshaft fillet. Therefore, no energy data related to the process could be extracted.

The study performed by (Spiteri, Ho, and Lee 2007) developed a three-dimensional numerical model to evaluate the influence of crankshaft deep rolling on the component's fatigue performance. However, according to the authors, due to restrictions in computational time, the simulation was simplified and the full rolling load profile was not applied, what prevents the extraction of reliable information about energy output.

Studies related to deep rolling that includes numerical simulations, but are not specifically about crankshafts, are extensive. A state of the art review in the field was summarized by (Delgado et al. 2016). It highlights that most numerical models simplify the workpiece geometries and, consequently, the applied boundary conditions. Investigations such as (Perenda, Trajkovski, and Andrej 2015; Trauth et al. 2013) all considered only a section of the component under study. The research made by (Hassani-gangaraj, Carboni, and Guagliano 2015) modeled a portion of a railway axle as a flat surface under deep rolling. A holistic understanding on the process parameters enabled an optimization of the process for component's enhanced fatigue performance. However, still no remarks on the energy output was highlighted or even mentioned.

Probably the only research to fully apply all deep rolling real process boundary conditions to crankshafts was summarized by (M. C. Cevik, Hochbein, and Rebbert 2012). By neglecting dynamic effects because of the low process speed, an implicit formulation was selected. Also, no information on energy output was published.

Energy output is most commonly analyzed in researches related to impact events such as drop tests and projectiles specimens. Examples of such studies are depicted in (Ali, M. Qamhiyah, A. Flugrad, D. Shakoore 2008; Tanlak, Sonmez, and Talay 2011). The authors evaluated the energy outputs and could make a direct correlation to the sequence

of events. The kinetic energy drop and internal energy rise means that the impact is occurring and the energy is being converted into material plastification. Artificial energy was also assessed, as it gives an indication on the amount of energy dispensed to stabilize the computational process rather than to simulate the physical process (Tanlak, Sonmez, and Talay 2011). The research performed by (Prior 1994) discusses techniques to simulate metal forming process and analyzes the ratio between kinetic and internal energies. The authors state that a general rule of thumb to maintain the problem with a quasi-static nature is to restrain the kinetic to about 5% of the internal energy. Studies related to forming process such as (Mohebbi and Akbarzadeh 2010; Wong, Dean, and Lin 2004) also cares for the energy balance, since it dictates whether the simulation is physically representative or not.

This survey on the state-of-the-art reveals that two-dimensional deep rolling models allow a first estimation of the process parameters, but they are unable to give sufficient information on the process dynamics, since no reliable energy output can be extracted. Regarding the development of three-dimensional models for crankshaft deep rolling, a gap still exists on the energy output evaluation. An opportunity opens to correlate model energy balance with the expected physical process at real operating conditions.

1.1 Objective and Approach

Based on the observed technological knowledge gap, the objective of this research is to analyze the energy output from deep rolling finite element (FE) simulations and correlate it with the process dynamics. This will give insight into the model representativeness of reality through data that is usually not explored in common simulations, but can still give indicatives on the model correctness.

The steps toward model development are briefly covered. Crankshaft geometry simplifications, material model selection, meshing, boundary and contact conditions are presented here. The impacts of the modeling options are evaluated through energy analyses. The proposed model was also subject to validation through fillet radii geometry and residual stress measurements. However, such discussion is not of interest here and will be addressed in future investigations.

2. COMPUTATIONAL PROCEDURE

The workflow in Figure 1 summarizes the model development process, performed with the finite element software ABAQUS®. Model geometry simplifications had to be considered and boundary conditions were imposed according to process dynamics. The simplified approach took into account all the relevant aspects of the real deep rolling process.

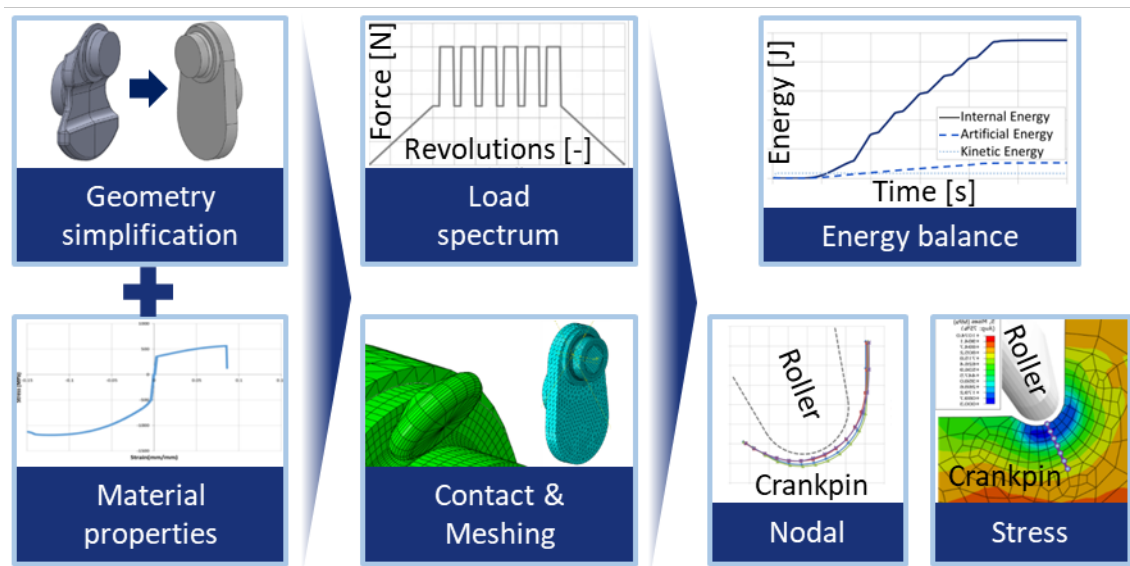


Figure 1. Model development workflow.

2.1 Geometrical simplifications

The first model simplification takes into account crankshaft symmetry. A fraction of 1/8 of the crankshaft was used to fully represent the component. This simplification has major impact on computational burden, since it permits the study of just one bearing. Important considerations are related to the original geometry of the half crank model. Details on webs, oilways and counterweights have little to no influence over the region of interest. This can be seen in the upper

left image present in Figure 1. Inertial and stiffness properties along the three axes of the simplified model were kept within 5% of the original crankshaft geometry.

2.2 Material model

Deep rolling simulation demands an elastic-plastic material model, for it induces severe material plastification. The subject under study is a spheroidal cast iron crankshaft, making ABAQUS® “Cast Iron Plasticity” (Dassault Systèmes 2011) a suitable model to be used, as stated by (M. C. Cevik, Hochbein, and Rebbert 2012). Data obtained from tensile and compression tests made with crankshaft cast iron served as input for the material model.

A simplification was assumed for the roller. As this component is not the main subject under study here, it was decided to model it as perfectly rigid solid. Future studies can take into account roller stiffness and resistance on deep rolling results.

2.3 Boundary conditions

Main boundary conditions for a deep rolling simulation relate to process inputs. Number of revolutions, rolling load, roller angle and force application profile were set accordingly to real deep rolling parameters. Symmetry conditions were set to restrict displacement in the Z axis of the transverse sections of the crankpin and main journal, as shown in Figure 2.

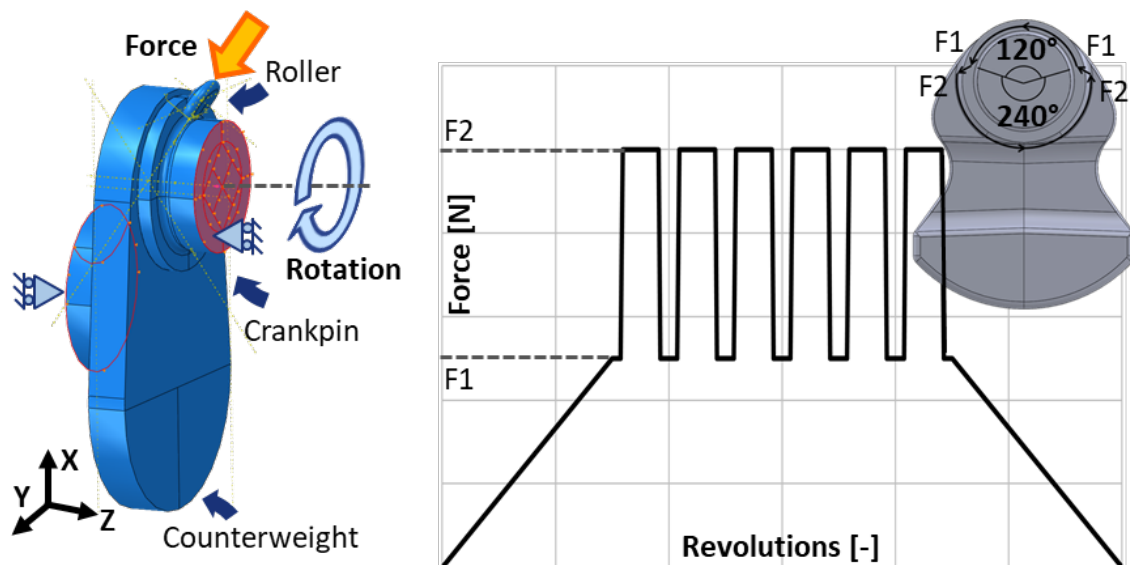


Figure 2. Boundary conditions applied to the model under development.

Rolling force application at the crankpin follows the profile shown in Figure 2. Loading and unloading steps relate to the fillet region that is being strain hardened. Higher loads are needed at the crankpin fillet bottom, since this area suffers tractive stresses under bending when the engine is operating, which can eventually lead to fatigue failure. In order to model the process kinematics, the roller was fixed in all degrees of freedom, except in the direction of force application and the crankpin was set to rotate around it.

2.4 Meshing

Since the analysis should aggregate reliable results with relatively low computational burden, two different element types were used for the half crank model. Web, counterweight and main bearing were coarse meshed with first order tetrahedrons, as shown in Figure 3a. As noted by (M. C. Cevik, Hochbein, and Rebbert 2012), this choice does not affect simulation results at the fillet area, as it is far enough from rolling load application. Fillet and pin bearing regions, of most importance in the analysis, were discretized by first order hexahedrons with reduced integration, as suggested by (C. Cevik 2011) and (Balland et al. 2013). Figure 3b illustrates the fine mesh proposed at the fillet area. The two mesh regions with different types of elements were coupled through ABAQUS® tie feature.

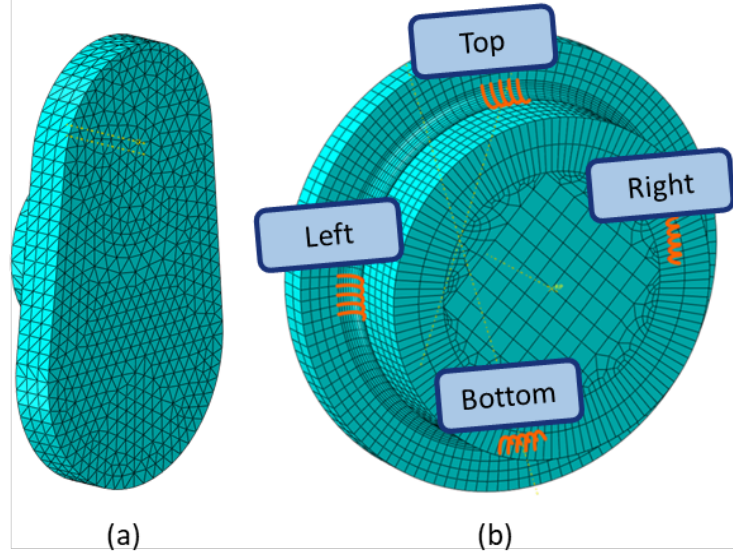


Figure 3. Mesh characteristics: (a) coarse at the web/counterweight/main journal; (b) fine at the crankpin fillet radius highlighted at crankpin region.

As did (Barge, M. Hamdi, H. Rech, J. Bergheau 2005) to prevent element hourglass modes in their machining simulations, artificial stiffness was implemented through enhanced hourglass control. In the same direction, an Arbitrary Lagrangian Eulerian (ALE) adaptive mesh feature was used to avoid severe mesh distortions. Acceptable level of Artificial Energy is suggested to stay within 10% of Internal Energy (Dassault Systèmes 2011).

2.5 Numerical formulation

This model simulates the real process duration. The studies of (Trauth et al. 2013) and (Tanlak, Sonmez, and Talay 2011) used explicit formulations because of its suitability to solve problems with complex contact interactions and dynamic behavior. The greatest challenge with this option is to develop a fine mesh and still maintain practical computational time. An explicit solver is considered robust because it does not work with a stiffness matrix at every increment or is iterative, differently from an implicit formulation. As explained by (Bathe 1996), the problem is solved by computing, at each step, dynamic equilibrium equations using dynamic relaxation. It begins by accounting for the initial conditions, such as velocity and predefined stress fields. Then, through the central difference method at every step, it calculates accelerations, nodal velocities, displacements, strains and, ultimately, update stresses. After that, it computes the internal forces and residual force vector. That is why, so that the model can converge, the critical time step must be small (Bathe 1996). The critical time step is basically determined in Eq. (1) as follows.

$$\Delta t = L^e / c_d \quad (1)$$

Time increment Δt is equal to the ratio between the smallest element length L^e and speed of sound in the given material c_d . As it is stated by (Bathe 1996), c_d can be calculated using Eq. (2).

$$c_d = (E / \rho)^{1/2} \quad (2)$$

The relationship between Young modulus E and density ρ is important, because it allows the possibility of altering time increment artificially. This technique is called mass scaling and can be applied to the whole model at the beginning of each analysis step. Altering density by a factor of ρ^2 changes the stable time increment by a factor of ρ .

In this particular study, mass scaling was implemented to increase time increment and speed up the simulation. Caution was taken, however, not to let inertial effects dominate the analysis and transform a quasi-static into a dynamic problem. To evaluate if spurious effects appear, the balance between Internal and Kinetic Energies should be at 5%, up to a maximum of 10% (Dassault Systèmes 2011). Energy balance is defined in Eq. (3).

$$E_I + E_{FD} + E_{KE} + E_V - E_W = E_{TOTAL} = constant \quad (3)$$

In a common quasi-static analysis, a great fraction of work done by external loads E_W should be transformed into internal energy E_I . A part of this work can be dissipated through frictional energy E_{FD} and viscous energy E_V . If the

kinetic energy E_{KE} reaches high values compared with internal energy, it means that dynamic aspects are dominating the model and some adjustments must be made. Typically, the value of kinetic energy should not exceed 10% of internal energy in quasi-static analyses as explained in (Dassault Systèmes 2011). The procedure adopted, then, was to scale the mass artificially as much as possible maintaining the kinetic energy at restrained levels. Total energy E_{TOTAL} should be fairly constant, with an error of approximately 1% (Dassault Systèmes 2011).

Internal energy is composed by elastic strain E_E , plastic strain dissipation E_{PD} and artificial energy E_A , usually related to control deformation modes with zero energy called hourglassing. Viscoelasticity E_{CD} , damage E_{DMD} , distortion control E_{DC} and fluid cavity E_{FC} energies are all zero in the analysis under development. Equation (4) summarizes the internal energy calculation.

$$E_I = E_E + E_{PD} + E_A + E_{CD} + E_{DMD} + E_{DC} + E_{FC} \quad (4)$$

Other than applying mass scaling to the model, one can decrease computational time by changing the load rate. For deep rolling simulation, this means increase the half crank rotational velocity.

Summarizing, mass scaling was chosen properly so that, at the same time, simulation time is practical and the ratio between internal and kinetic energies falls into the expected range. Energy balance analysis will be treated in the Results and Discussion section to justify all choices in terms of mass scaling increase.

3. RESULTS AND DISCUSSION

3.1 Finite element simulation results

Strain and stress field outputs were evaluated for the converged mesh model using ABAQUS®'s post-processor. The results appear to be qualitatively in agreement with expectations, as can be observed in the contour graphs of a crankpin transverse cut in Figure 4. The top region, which experiences less rolling load, presents lower strain and Von Mises stress levels.

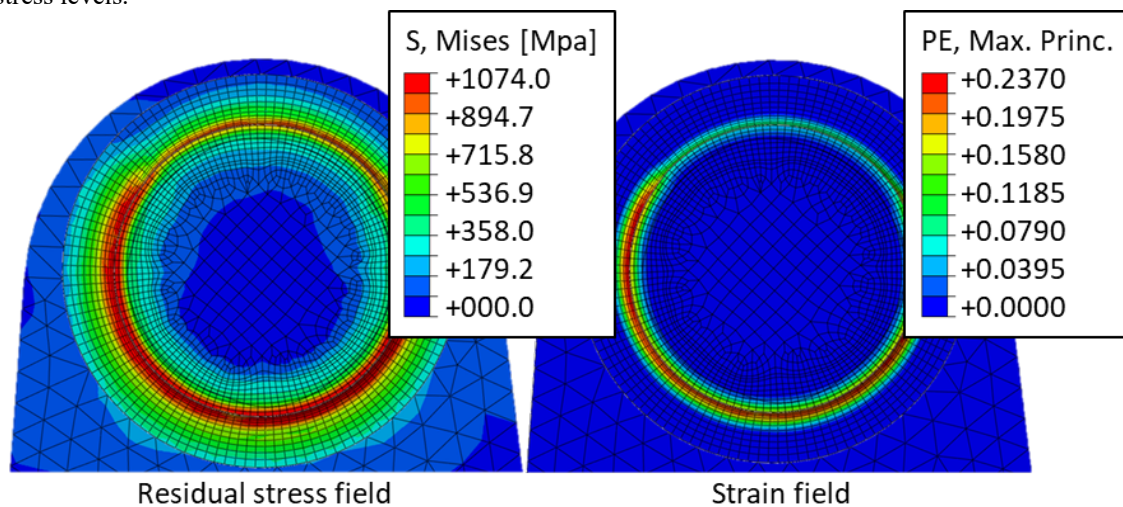


Figure 4. Transverse cut in the proposed model to show final Von Mises stress and plastic strain states.

3.2 Energy balance analysis

The first aspect analyzed in this section is the total energy data, which is compared with internal energy. In a numerical model, the sum of all energies created and external work should be fairly constant. As can be seen in

Figure 5, total energy in comparison with internal energy lies inside a 0.5% margin. This information is important to assure that the model does not have any major errors and the analysis is running correctly.

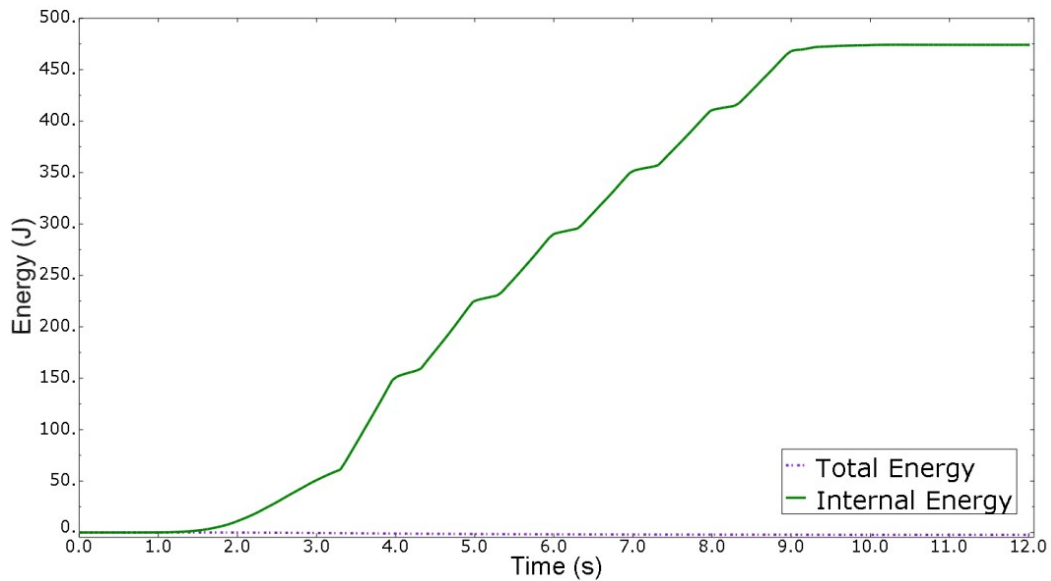


Figure 5. Total and internal energies comparison.

Energy output had an important role to help setting a suitable mass scaling factor for the model. As commented in section 2.5, a simulation using an explicit code can lead to long computational time to be solved. Without mass scale, a deep rolling FE simulation was estimated to last weeks. Proper artificial density factor was then chosen. As one can infer, altering the model’s mass has an impact on kinetic energy, since one is directly proportional to the other. With that stated,

Figure 6 shows that care was taken to maintain the kinetic energy within 5% of internal energy. This ensures that the dynamic aspect is not governing the analysis and it remains with its quasi-static nature.

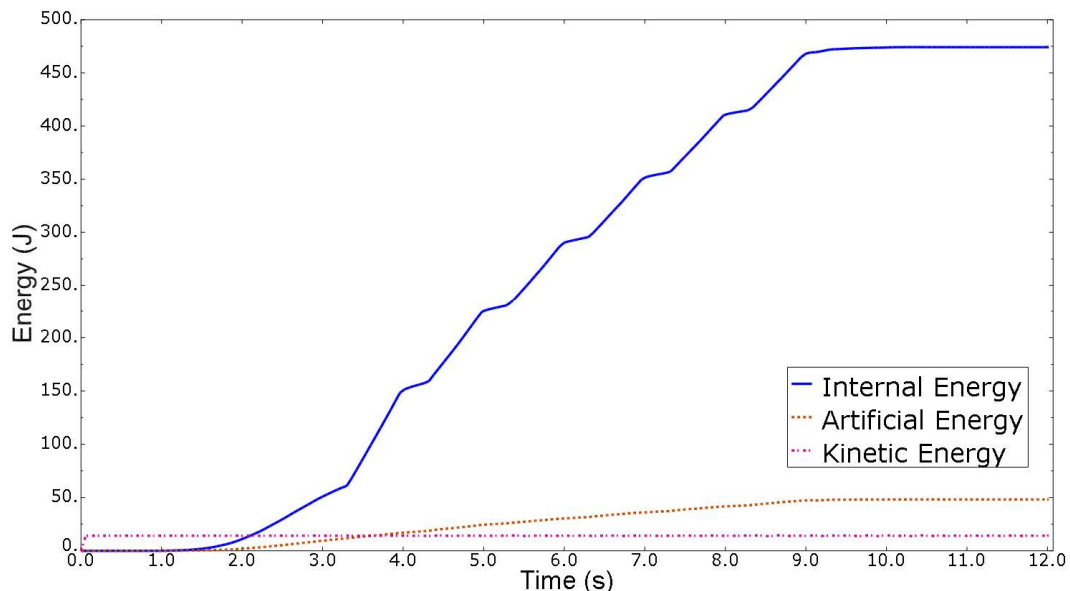


Figure 6. Comparison between internal, artificial and kinetic energy for one simulation.

Figure 6 shows the relation between internal and artificial energies. One can see that artificial energy reaches levels near 10% of internal energy. Mesh refinement should reduce the energy directed to contain hourglassing (Barge, M. Hamdi, H. Rech, J. Bergheau 2005; Dassault Systèmes 2011).

Together with internal energy, Figure 7 brings elastic strain and inelastic dissipation energies. The last one is the fraction of the internal energy which is dissipated through inelastic processes such as plasticity (Dassault Systèmes

2011). The elastic fraction summed with inelastic and artificial energies results in total internal energy. One can observe the results of rolling force profile, which was depicted in Figure 2 and is miniaturized in Figure 7. Until three seconds the force is still ramping up. After this point, a full and half load pattern begin to alternate up to nine seconds of simulation time. This has an effect that can be seen both in the internal energy and in inelastic dissipation energy curves. Regions of full load are characterized by a higher slope and a longer period of time. Half load periods still have a visible positive slope, but are shorter and less steep. Interesting to notice is also the decrease in the slope as the cycles pass by, from three up to nine seconds. Figure 7 brings a clarification on that matter. The slope α corresponding to the first full load is clearly steeper than slope β , the last full load. This is proof that the deep rolled fillet material is suffering strain hardening. Even with the same amount of force, the roller cannot deform the material by the same rate. Elastic strain energy practically stays at a constant level throughout the whole simulation.

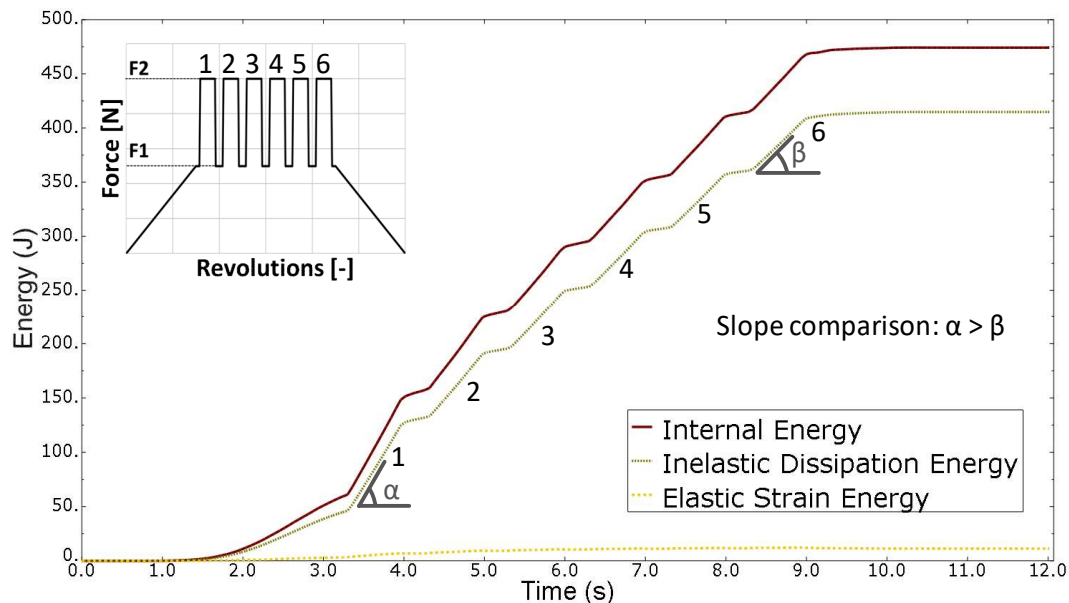


Figure 7. Comparison between internal, inelastic dissipation and elastic strain energies.

4. CONCLUSIONS

Energy output, commonly overlooked in most simulation analysis, can bring interesting information in terms of model response. The following can be outlined as conclusions of this research:

- Deep rolling strain hardening could be observed in the inelastic dissipation energy curve.
- Dynamic effects were evaluated in terms of kinetic and internal energies and conclusions could be drawn to confirm that the model indeed simulates a quasi-static event.
- Action taken towards reducing processing time was related to mass scaling. One must always keep in mind that proper selection should be a concern in order to achieve satisfactory results.

Further publications will follow, encompassing the evaluation of different mesh refinements in terms of energy balance. Validation of the model's strain and residual stress outputs is also being performed. This study is ongoing to correlate the residual stress state with the crankshaft fatigue strength and life. In order to accomplish that, a torsion and bending resonant fatigue test rig is in its development final stages. The ultimate goal of the research is to understand how the residual stress state influences the crankshaft fatigue life. This should be done by evaluating residual stress and fatigue strength of crankshaft prototypes with different deep rolling parameters. If such correlation can be reached, a validated deep rolling finite element model should greatly improve and benefit crankshaft engineering. Optimal process parameters could be selected during component design to enhance fatigue strength and performance in terms of weight and inertia.

5. ACKNOWLEDGEMENTS

This study was partially funded by the Brazilian agency CNPq under grants 159026/2013-0 and 300886/2013-6. The authors would like to thank MSc. Paulo Vieira Netto (FCA Group) for the enlightening discussions and contributions.

6. REFERENCES

- Ali, M. Qamhiyah, A. Flugrad, D. Shakoor, M. 2008. "Theoretical and Finite Element Study of a Compact Energy Absorber." *Advances in Engineering Software* 39: 95–106.
- Balland, Pascale, Laurent Tabourot, Fabien Degre, and Vincent Moreau. 2013. "Mechanics of the Burnishing Process." *Precision Engineering* 37(1): 129–34. <http://dx.doi.org/10.1016/j.precisioneng.2012.07.008>.
- Barge, M. Hamdi, H. Rech, J. Bergheau, M. 2005. "Numerical Modelling of Orthogonal Cutting: Influence of Numerical Parameters." *Journal of Materials Processing Technology* 164–165: 1148–53.
- Bathe, K. J. 1996. *Finite Elements Procedures*. Upper Saddle River, New Jersey: Prentice-Hall.
- Cevik, Cagri. 2011. "An Efficient Methodology for Borderline Design of Crankshafts." RWTH Aachen.
- Cevik, M Cagri, Helmut Hochbein, and Martin Rebbert. 2012. "Potentials of Crankshaft Fillet Rolling Process." *SAE Technical Papers*.
- Chien, W. Y., J. Pan, D. Close, and S. Ho. 2005. "Fatigue Analysis of Crankshaft Sections under Bending with Consideration of Residual Stresses." *International Journal of Fatigue* 27(1): 1–19.
- Choi, K. S., and J. Pan. 2009. "Effects of Pressure-Sensitive Yielding on Stress Distributions in Crankshaft Sections under Fillet Rolling and Bending Fatigue Tests." *International Journal of Fatigue* 31(10): 1588–97.
- Choi, K S, and J Pan. 2005. "Effects of Roller Geometry on Contact Pressure and Residual Stress in Crankshaft Fillet Rolling." *SAE Technical Paper Series (724)*.
- Dassault Systèmes. 2011. ABAQUS® CAE User's Manual *Abaqus 6.11*.
- Delgado, P, I I Cuesta, J M Alegre, and A Díaz. 2016. "State of the Art of Deep Rolling." *Precision Engineering* 46: 1–10. <http://dx.doi.org/10.1016/j.precisioneng.2016.05.001>.
- Hassani-gangaraj, S M, M Carboni, and M Guagliano. 2015. "Materials & Design Finite Element Approach toward an Advanced Understanding of Deep Rolling Induced Residual Stresses , and an Application to Railway Axles." *Materials & Design* 83: 689–703. <http://dx.doi.org/10.1016/j.matdes.2015.06.026>.
- Mohebbi, M S, and A Akbarzadeh. 2010. "Journal of Materials Processing Technology Experimental Study and FEM Analysis of Redundant Strains in Flow Forming of Tubes." *Journal of Materials Processing Technology* 210: 389–95.
- Perenda, Jasenko, Jovan Trajkovski, and Z Andrej. 2015. "Journal of Materials Processing Technology Residual Stresses after Deep Rolling of a Torsion Bar Made from High Strength Steel." *Journal of Materials Processing Technology* 218: 89–98.
- Prior, A.M. 1994. "Materials Processing Technology." *Journal of Materials Processing Technology* 45(X): 649–56.
- Spiteri, Paul, Simon Ho, and Yung L. Lee. 2007. "Assessment of Bending Fatigue Limit for Crankshaft Sections with Inclusion of Residual Stresses." *International Journal of Fatigue* 29(2): 318–29.
- Tanlak, N., F. Sonmez, and E. Talay. 2011. "Detailed and Simplified Models of Bolted Joints under Impact Loading." *The Journal of Strain Analysis for Engineering Design* 46(3): 213–25.
- Trauth, Daniel, Fritz Klocke, Patrick Mattfeld, and Andreas Klink. 2013. "Time-Efficient Prediction of the Surface Layer State after Deep Rolling Using Similarity Mechanics Approach." *Procedia CIRP* 9: 29–34. <http://dx.doi.org/10.1016/j.procir.2013.06.163>.
- Wong, C C, T A Dean, and J Lin. 2004. "Incremental Forming of Solid Cylindrical Components Using Flow Forming Principles." *Journal of Materials Processing Technology* 154: 60–66.

7. RESPONSIBILITY NOTICE

The authors are the only responsible for the printed material included in this paper.